A Physical-Chemical Study of Biological Iron Transport Mediated by Proteins and Low Molecular Weight Chelators

Suraj Dhungana
Duke University

Iron in a biological system is extremely well regulated. Mammalian and microbial cells utilize iron-transport proteins and iron specific chelators to acquire iron from their environment. The ligands present in the first coordination shell chelate iron very tightly to prevent its hydrolysis and precipitation. These ligands are also responsible for controlling the Fe^{3+}/Fe^{2+} redox potential. Redox potential control is of importance because the time and site-specific delivery of iron may be achieved by redox facilitated ligand exchange. Control over the redox potential prevents unnecessary or premature release and/or ligand scrambling of the essential nutrient iron.

Mammalian Iron Transport[1]

Transferrin (*h*Tf), the iron transporter in mammals, is a bilobal protein with a single iron-binding site in each lobe (Figure 1). Iron is borne by *h*Tf as Fe^{3+}, with a reduction potential too low (< -500 mV) for it to be reduced to Fe^{2+} by physiological means, either at extracellular pH (7.4) or at endosomal pH (5.6). Iron exits the endosome, to which it is internalized by the iron-dependent cell, via the membrane divalent metal ion transporter known as DMT1, which accepts iron only as Fe^{2+}. Although once released from *h*Tf iron is easily reducible, the time required for release as Fe^{3+} to physiological chelators, even at endosomal pH, is long (>6 min) compared to the cell-cycling time of transferrin, which may be as little as 1-2 min. A fundamental problem in understanding intracellular iron metabolismis how iron is released from *h*Tf to cross the endosomal membrane for access to the cytoplasm. A salient feature of the transferrin-to-cell cycle in iron is the persistence of the transferrin-transferrin receptor complex throughout the cycle. The possibility that the transferrin receptor modulates the reduction potential of transferrin-bound iron was therefore investigated.

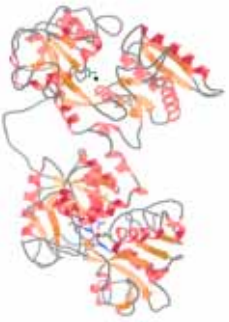

Figure 1: Ribbon diagram of mammalian transferrin

[1] From publication 5 in author's bio-sketch and Chapter 2 of the dissertation. For work cited please refer to the publication and the references within.

The reduction potentials of iron in the C-terminal lobe of *h*Tf complexed to its receptor, at extracellular pH and at endosomal pH, were measured. At pH 7.4 the C-lobe in its complex with receptor exhibited a similar reduction profile as the C-lobe in receptor-free full-length *h*Tf, <-500 mV, and therefore is inaccessible to physiological reductants. Although the energetics of Fe^{3+} reduction in free *h*Tf are almost identical at pH 7.4 and pH 5.8, with reduction potentials near -520 mV in both cases, the energy cost of reduction in C-lobe complexed to receptor is greatly decreased by the receptor-induced rise in reduction potential to -289 mV, comparable to that of the pyridine nucleotides, -284 mV (Figure 2). Fe^{2+} is bound by *h*Tf at least 14 orders of magnitude more weakly than Fe^{3+}, so that reductive release of iron bound to *h*Tf in the transferrin-transferrin receptor complex is physiologically and thermodynamically feasible, and the barrier to transport across the endosomal membrane is lifted. The transferrin receptor, therefore, is more than a simple conveyor of transferrin and its iron.

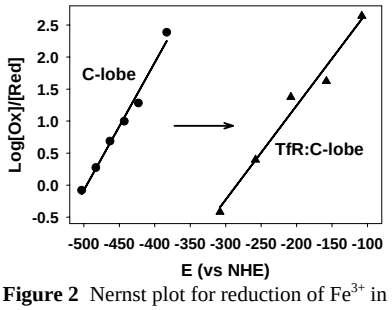

Figure 2 Nernst plot for reduction of Fe^{3+} in the C-lobe of human transferrin, free and complexed to the transferrin receptor, at endosomal pH 5.8.

Ferric Binding Protein Mediated Bacterial Iron Transport[2]

A periplasmic iron binding protein called ferric binding protein (Fbp) is responsible for shuttling iron across the periplasmic space of certain Gram-negative bacteria. Fbp is also referred to as a bacterial transferrin because of its structural and functional similarities to mammalian transferrin (Figure 3 and 4). In spite of these remarkable similarities, differences between iron binding by transferrin and Fbp exist.

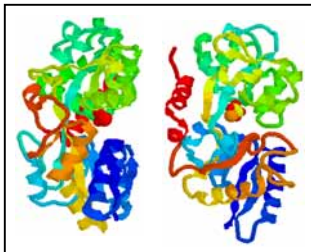

(a) **(b)**

Figure 3 Ribbon diagran of (a) Fbp and (b) C-lobe of mammalian transferrin

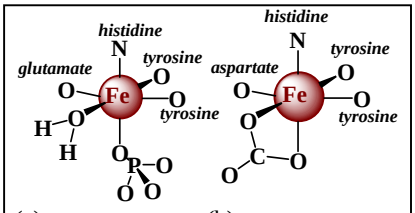

(a) (b)

Figure 4 First coordination shell of (a) Fbp with phosphate as synergistic anion (b) transferrin with carbonate as synergistc anion

While the presence of an exogenous anion is a requirement for Fe^{3+} binding by *n*Fbp, we have established that the identity of the anion is not specific *in vitro*. *n*Fbp was reconstituted as a stable iron containing protein utilizing a number of exogenous anions present in the recombinant form of the protein (arsenate, citrate, NTA,

[2] From publications 3, 8 and 12 in author's bio-sketch and dissertation Chapters 3, 4 and 5. For work cited please refer to the publications and the references within.

pyrophosphate, oxalate, sulfate), in addition to phosphate.. The affinity of the protein for Fe^{3+} is anion dependent, as evidenced by the effective Fe^{3+} binding constants K'_{eff} (Table 1). The redox potentials for Fe^{3+}*n*FbpX/Fe^{2+}*n*FbpX reduction are also found to depend on the identity of the synergistic anion required. Facile exchange of exogenous anions (Fe^{3+}*n*FbpX + X' ➔ Fe^{3+}*n*FbpX' + X) is established and provides a pathway for environmental modulation of the iron chelation and redox characteristics of *n*Fbp. These findings allow us to propose an iron transport mechanism facilitated by Fbp as summarized in Figure 5.

Table 1 Ferric Binding Protein Characterization for Different Exogenous Anions

Fe^{3+}*n*FbpX X^{n-} =	$[X^{n-}]_{50}$ / M [a]	Relative Affinity [b]	λ_{max} /nm (ε/$M^{-1}cm^{-1}$)	K'_{eff} / M^{-1}	$E_{1/2}$ / mV (NHE)
Phosphate	1.0×10^{-6}	1.0	481 (2430)	4.2×10^{18}	-300
Arsenate	7.9×10^{-6}	0.15	476 (2280)	1.3×10^{18}	-251
Pyrophosphate	9.5×10^{-6}	0.13	472 (2770)	1.9×10^{17}	-212
NTA	2.3×10^{-4}	0.0052	468 (3460)	2.2×10^{17}	-184
Citrate	3.5×10^{-4}	0.0034	474 (1770)	1.4×10^{17}	-191
Oxalate	4.2×10^{-4}	0.0029	475 (3570)	3.7×10^{17}	-186
Carbonate	2.4×10^{-2}	0.000050	-	-	-

[a]Concentration of anion required to displace 50% of bound PO_4^{3-} from Fe^{3+}*n*FbpPO$_4$.
[b]Binding affinity of various X^{n-} for Fe^{3+}*n*Fbp to form Fe^{3+}*n*FbpX relative to X^{n-} = PO_4^{3-}.

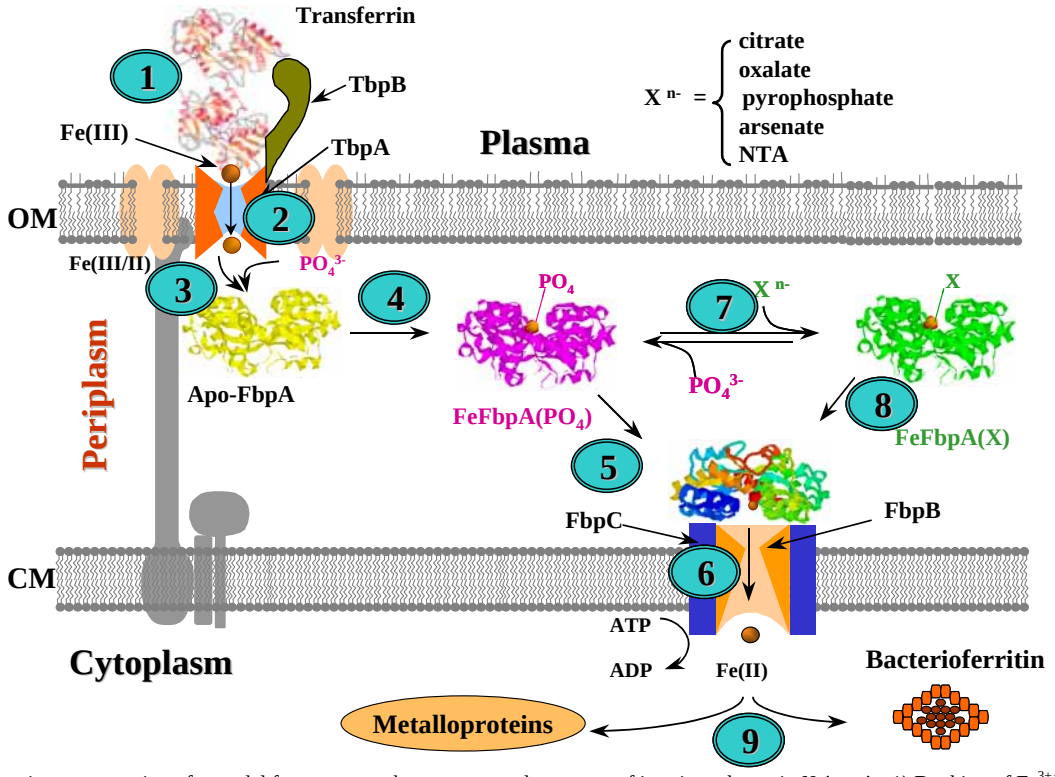

Figure 5 Schematic representation of a model for outer membrane to cytosol transport of iron in pathogenic *Neisseria* 1) Docking of Fe^{3+}*h*Tf at the outer membrane receptor and reduction of bound Fe^{3+} to Fe^{2+}. 2) Release of Fe^{2+} from *h*Tf and movement to interior side of the membrane receptor. 3) Sequestration of Fe^{2+} by *n*Fbp in the presence of phosphate. 4) Oxidation of Fe^{2+}*n*Fbp(PO_4). 5) Movement of Fe^{3+}*n*Fbp(PO_4) across the periplasmic space. 6) Docking of Fe^{3+}*n*Fbp(PO_4) at the inner membrane receptor and reduction of bound Fe^{3+} to $Fe^{2+}$and release of Fe^{2+} and passage through the cytoplasmic membrane receptor into the cytosol. 7) Exchange of phosphate exogenous anion by citrate to form Fe^{3+}*n*Fbp(Cit). 8) Docking of Fe^{3+}*n*Fbp(Cit) at the inner membrane receptor and reduction of bound Fe^{3+} to Fe^{2+} and release of Fe^{2+} and passage through the cytoplasmic membrane receptor into the cytosol.

The kinetics of iron release from various forms of holo-FbpA (Fe^{3+}FbpA-X; X = PO_4^{3-} and NTA) was studied during the course of a chelator competition reaction using EDTA and Tiron.

Competing chelators can effectively remove Fe^{3+} from Fe^{3+}FbpA-X and control the mechanism and the rates of the exchange kinetics. This ability of the synergistic anion to modulate the kinetics of Fe^{3+} release along with its ability to modulate the thermodynamics of Fe^{3+} release further establishes the synergistic anions as crucial players in periplasmic Fe^{3+} transport in Gram-negative bacteria.

Additionally, we were able to study the kinetics and mechanism of *p*-nitrophenyl phosphate ester (NPP) hydrolysis catalyzed by FbpA by noting that NPP will act as a synergistic anion by displacing labile sulfate from Fe^{3+}FbpA-SO_4. Formation of Fe^{3+}FbpA-NPP was found to accelerate the rate of hydrolysis of the bound phosphate ester (k_{hyd} = 1.6 x 10^{-6} s^{-1}) by >10^3 fold over the uncatalyzed reaction. The overall reaction scheme investigated is shown in Scheme 1. These findings suggest a dual function for FbpA *in vivo*: transport of Fe^{3+} across the periplasmic space to the inner membrane in certain Gram-negative bacteria and hydrolysis of periplasmic polyphosphates.

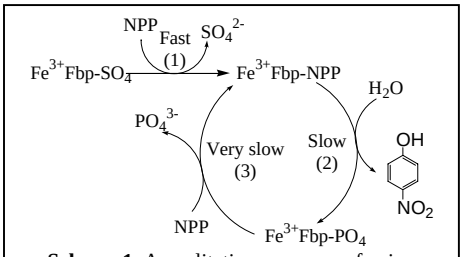

Scheme 1 A qualitative summary of anion exchange and hydrolysis reactions by FbpA.

Siderophore Mediated Microbial Iron Transport[3]

A vast number of microbes are non pathogenic and need to acquire iron from diverse sources. This includes environmental $Fe(OH)_3$ that limits the total solubility of iron to 10^{-10} M. These microbes utilize a different and more versatile iron acquisition strategy involving siderophores. Siderophores exhibit a high (log β > 30) and specific affinity for selective chelation of Fe^{3+} in the presence of other environmentally prevalent metal ions.

Several siderophores and siderophore analogs (Figure 6) were investigated for their

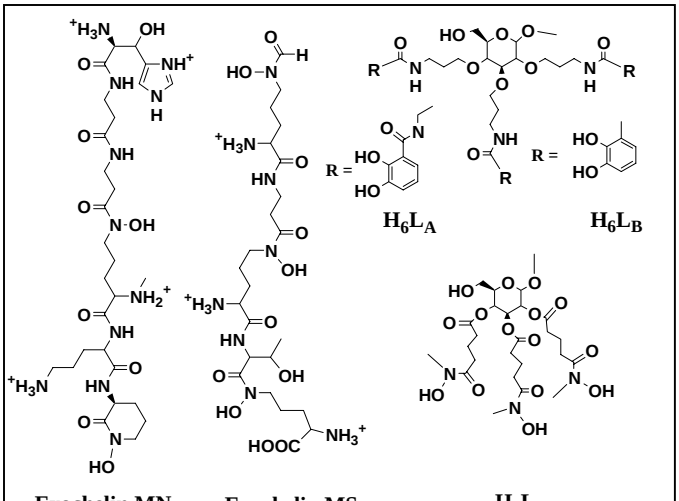

Figure 6 Siderophore and siderophore mimic structures discussed in the text

[3] From publication 1, 7, 9 and 10 in author's bio-sketch and dissertation Chapters 6, 7, 8 and 9. For work cited please refer to the publications and the references within.

Fe^{3+} chelation/dechelation properties in the context of an overall siderophore mediated iron acquisition scheme. Thermodynamic parameters determined for the Fe-complexes of these siderophores and analogs are summarized in Table 2. The very high Fe^{3+} binding affinity and a high pFe of exochelins and the saccharide based synthetic analogs are suggestive of these molecules being effective chelating agents at physiological conditions.

Table 2 Thermodynamic Parameters for Fe-Complexes

Siderophore and Siderophore Analogs	Log β[a] Fe^{3+}	Log β[a] Fe^{2+}	pFe[b]	$E_{1/2}$ vs NHE[b] (mV)
Saccharide H_3L_A	31.9	12.1	27.1	-436
Exochelin MN	39.12	16.7	31.1	-595
Exochelin MS	28.9	10.1	25.0	-380
Saccharide H_6L_A	41.4	--	28.6	--
Saccharide H_6L_B	46.4	--	28.3	--

[a] Defined as $\beta_{xyz} = [Fe_xL_y]/[Fe]^x[L]^y$ for $xFe + yL \rightleftharpoons Fe_xL_y$. L represents the fully deprotonated form of the siderophore.
[b] $-\log[Fe^{3+}]$ at $[Fe(III)]_{tot} = 10^{-6}$ M, $[L]_{tot} = 10^{-5}$ M and pH = 7.4.

Molecular Recognition of Fe(III)-siderophore Complexes[4]

Structural studies of a family of siderophores allow us to understand the key components behind the recognition mechanism. A well-studied siderophore, ferrioxamine B, was crystallized (Figure 7). The crystal structure contains a racemic mixture of Λ-N-*cis, cis* and Δ- N-*cis, cis* coordination isomers. The structural parameters and the conformational features of ferrioxamine B compare very well with those of ferrioxamine D_1 and E with an exception of the orientation of the pendant protonated amine, which is pointing away from the connecting amide chains and towards the carbonyl face of the inner coordination shell distorted octahedron.

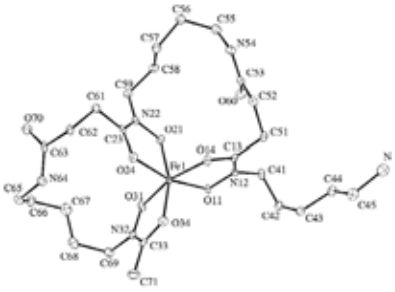

Figure 7 A perspective single-molecule drawing of ferrioxamine B

Ionophore-siderophore host-guest assemblies comprised of 18-crown-6, benzo-18-crown-6, and *cis-syn-cis*-dicyclohexano-18-crown-6 with ferrioxamine B were successfully crystallized and their structures were determined by single-crystal X-ray diffraction (Figure 8). The structures confirm the ability of the crown ether cavity to recognize ferrioxamine B through second coordination sphere host-guest complexation with 1:1 stoichiometry. The structural parameters for the ferrioxamine B molecule in all three crystal structures show a high degree of congruence and exclusively contain Δ-N-*cis,cis* and Λ-N-*cis,cis* isomers. This isomeric selectivity from the 16 possible isomers suggests that the Δ-N-*cis,cis*

[4] From publications 6 and 11 in author's bio-sketch and dissertation Chapters 10 and 11. For work cited please refer to the publications and the references within.

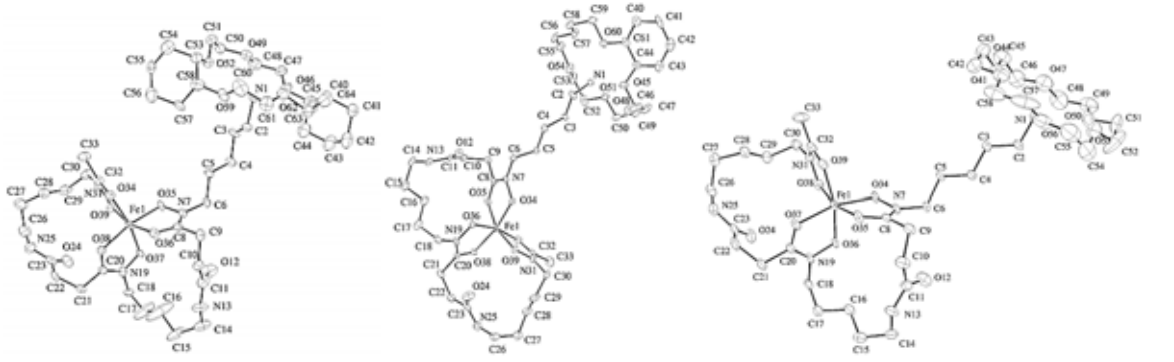

(a) **(b)** **(c)**

Figure 8 A perspective single-molecule drawing of (a) *cis*-*syn*-*cis*-dicyclohexano-18-crown-6**:**ferrioxamine B (b) benzo-18-crown-6**:**ferrioxamine B (c) 18-crown-6**:**ferrioxamine B host-guest assembly based on the crystal structure, showing atom numbering

and Λ-N-*cis,cis* isomers are possibly the lowest energy isomeric forms. The presence of the pendant protonated amine in the second coordination shell of ferrioxamine B is certainly capable of providing the ferrioxamine B with additional hydrogen bonding capabilities during the receptor recognition, and other smaller host molecule recognition. The orientation of the pendant protonated amine towards the more open carbonyl trigonal face of the first coordination shell of ferrioxamine B in these assemblies may also be of significance in the cell receptor recognition process, as the oxygen atoms on this face are available for intermolecular hydrogen bonding.

Fe(III) Release from High Affinity Fe(III)-Siderophore Complexes[5]

Redox facilitated release and delivery of iron is an attractive hypothesis for iron release from very stable Fe(III)-siderophore complexes. The reduction of Fe^{3+} to Fe^{2+} operates as a sensitive switch that makes the complex susceptible to protonation, and thermodynamically and kinetically facilitates the dissociation of iron. However, a key challenge in a biological system lies in the fact that Fe(III)-siderophore complexes have very negative redox potentials (Table 2) that are generally out of the range available to physiological and environmental reducing agents. Biological reduction of Fe(III)-siderophore complexes requires a positive shift in the conditional redox potential of Fe(III)-siderophore complexes into a range accessible to reducing cofactors like NADPH or NADH (-320 mV/NHE). Factors such as pH, lipophilicity of the medium, the presence of competing Fe^{2+}-chelators, and reduction of the denticity of the Fe(III)-complexed siderophore (Scheme 2), can all result in a positive shift in the

[5] From publications 1, 4, 7, 9 and 10 in author's bio-sketch and dissertation Chapters 6, 7, 8 and 9. For work cited please refer to the publications and the references within.

redox potential. Although the influence of these factors was studied separately, they most likely work concurrently and complement each other under environmental conditions. For example, to shift the redox potential of a $Fe(III)L_3$ (refer to Figure 6 for structure) complex from -436 mV (NHE) to ~ -300 mV (NHE) (in the redox range of NADPH or NADH) the pH must be lowered to ~5 (Figure 9), or a Fe^{2+} chelator needs to be present with $K_{Fe(II)L} > 10^{13}$. In an environmental system or cell compartment a pH lower than ~5 (*e.g.* endosomal pH) is difficult to attain, as is high concentrations of Fe^{2+} chelators with $K_{Fe(II)L} > 10^{13}$. However, these two factors can work together and bring about the required shift in the redox potential of the $Fe(III)L_A$ system and facilitate reduction under conditions that are representative of environmental or biological systems. Furthermore, factors such as lipophilicity of the medium and the denticity of the siderophore can also contribute towards shifting the redox potential positive. All of these factors help activate a redox switch that can modulate biological and environmental iron mobility and transport.

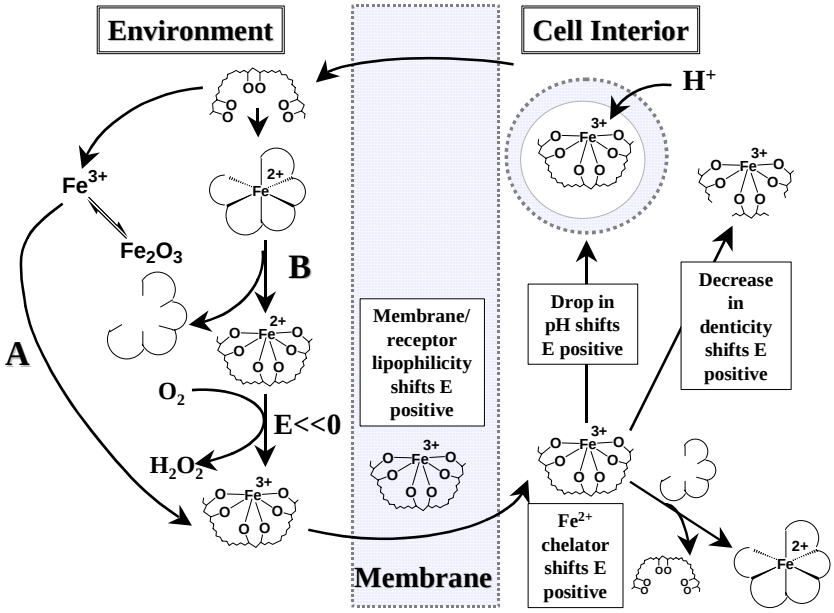

Scheme 2 Factors that shift the redox potential of Fe(III)-siderophore complex

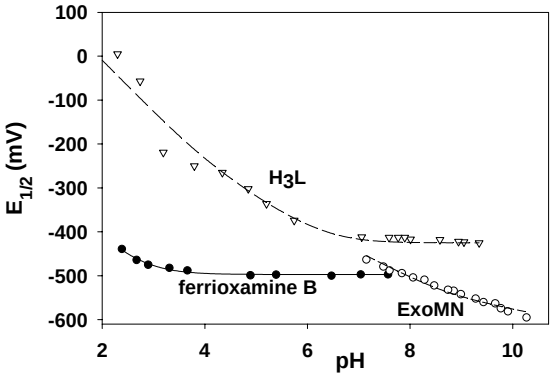

Figure 9 Redox potentials of Fe^{3+} complexes of siderophores and siderophore mimics as a function of pH.